Research Square

Preprints are preliminary reports that have not undergone peer review.
They should not be considered conclusive, used to inform clinical practice,
or referenced by the media as validated information.

Regulatory SH3-SH2 domain mutations in BCR–ABL1 drive imatinib resistance and confer dasatinib sensitivity in chronic myeloid leukemia

Samya Dey
Institute of Health Sciences, Presidency University https://orcid.org/0000-0003-3583-8551
Rumpa Mahata
BRIC-National Centre for Cell Science https://orcid.org/0000-0001-8026-1902
Sourav Pal
CSIR-Indian Institute of Chemical Biology
Koushik Saha
Institute of Health Sciences, Presidency University https://orcid.org/0009-0005-5559-9385
Soumi Basu
Saroj Gupta Cancer Centre & Research Institute
Debmalya Bhattacharyya
Saroj Gupta Cancer Centre & Research Institute
Dibyendu De
Balco Medical Centre
Deepam Pushpam
All India Institute of Medical Sciences
Rajib De
Nil Ratan Sircar Medical College
Tuphan Kanti Dolai
Nil Ratan Sircar Medical College
Arindam Talukdar
atalukdar@iicb.res.in

CSIR-Indian Institute of Chemical Biology
Manas Kumar Santra
manas@nccs.res.in

BRIC-National Centre for Cell Science
Somsubhra Nath
somsubhra.iha@presiuniv.ac.in

Institute of Health Sciences, Presidency University https://orcid.org/0000-0001-8214-1218

Research Article

Keywords: Chronic Myeloid Leukemia (CML), BCR:ABL1, Kinase domain (KD), Tyrosine Kinase Inhibitor (TKI), Imatinib-resistance, SH3-SH2 domain, Dasatinib

Posted Date: June 19th, 2026

DOI: https://doi.org/10.21203/rs.3.rs-9989394/v1

License: This work is licensed under a Creative Commons Attribution 4.0 International License. Read Full License

Additional Declarations: The authors declare no competing interests.

Abstract

Selection of second-line tyrosine kinase inhibitor (TKI) in chronic myeloid leukemia (CML) is largely guided by kinase domain (KD) mutations in BCR::ABL1; however, a substantial subset of imatinib-resistant cases (~ 40%) lack targetable KD alterations, limiting therapeutic stratification. Given the critical role of the Src homology 2 (SH2) and SH3 domains in regulating BCR::ABL1 activity, we investigated regulatory domain mutations in a cohort of CML with clinically-validated front-line imatinib resistance. Deep sequencing identified a *de novo* mutation pair, located in SH2 (Y167H) and SH3 (T117P) domain, in 16% cases. Following this, structure-guided molecular dynamics simulations indicated this mutation pair to destabilize the imatinib-compatible BCR::ABL1 conformation, resulting in reduced inhibitor engagement. Likewise, *in vitro* and *in vivo* experiments corroborated this non-responsiveness to imatinib. In contrast, computational and experimental analyses identified dasatinib as an effective second-line agent, restoring drug sensitivity despite the regulatory domain perturbations. Case studies further supported the efficacy of dasatinib in overcoming resistance associated with these mutations. Importantly, detection of this mutation pair in an independent validation set underscores the relevance of regulatory domain alterations as a previously under-recognized mechanism of TKI resistance. These findings advocate for routine interrogation of BCR::ABL1 regulatory domains to refine therapeutic decision-making in imatinib-refractory CML.

Introduction

Chronic myeloid leukemia (CML) is driven by BCR::ABL1 fusion oncoprotein, arising from the reciprocal translocation of chromosome 9 and 22 [t(9;22)(q34;q11)], cytologically known as Philadelphia chromosome (1). This constitutively-active tyrosine kinase sustains leukemogenesis through persistent activation of downstream signaling pathways (2, 3). The advent of tyrosine kinase inhibitors (TKIs), beginning with imatinib, has transformed CML into a manageable disease, with a 10-year overall survival of 83.3% for the patients in chronic phase (4). Mechanistically, imatinib stabilizes the inactive conformation of BCR::ABL1, thereby suppressing kinase activity and leukemic proliferation (5).

Despite these advances, therapeutic resistance remains a significant clinical challenge. Approximately one-quarter of patients exhibit suboptimal response or relapse on imatinib therapy (3). The most frequent mechanism involves point mutations within BCR::ABL1 kinase domain (KD; also referred as SH1 domain). A number of candidate mutations (eg. T315I gatekeeper mutation) are clinically validated, confirming their roles in emergence of drug-resistance, and, targetable with next-generation TKIs (6, 7). However, 30–40% of resistant cases lack candidate KD mutations, suggesting BCR::ABL1 mutation-independent or non-canonical resistance mechanisms, encompassing kinase overexpression, clonal evolution, and bypass signaling, remain poorly stratified and largely untargetable (6, 8, 9). Notably, the regulatory architecture of BCR::ABL1, particularly the Src homology 3 (SH3) and − 2 (SH2) domains that modulate kinase activation, has been underexplored in the context of resistance.

Structurally, BCR::ABL1 comprises multiple domains that cooperatively regulate its catalytic activity through intricate allosteric control mechanisms governing both active and auto-inhibited states (**Supplementary Fig. S1**) (9–11). The N-terminal portion harbors the SH3 and SH2 domains (12, 13), which are evolutionarily conserved protein–protein interaction modules. These domains are attached to KD through a flexible SH2-kinase linker region. The KD itself is bi-lobed in organization, consisting of a smaller N-terminal lobe (N-lobe) dominated by β-sheets and the αC-helix, and a larger C-terminal lobe (C-lobe), enriched in α-helices. Between the lobes lies the ATP-binding cleft, which serves as the catalytic core for phospho-transfer reactions. Several structural motifs within KD are functionally critical, including phosphate-binding loop (P-loop), activation loop (A-loop), αC-helix, a conserved Asp-Phe-Gly (DFG) motif at the N-terminus of A-loop and the gatekeeper residue Thr315 at the entrance of ATP-binding site (12, 14). Together, these elements orchestrate conformational transitions of BCR::ABL1, between active and inactive states. Mutations that perturb this regulation might reverse the inactive state to active state, causing inaccessibility to imatinib (10). A pioneer study from Michael W. Deininger's group identified a few SH3-SH2 domain mutations from a study cohort, and emphasized candidate mutations to destabilize the imatinib-competent auto-inhibited form of BCR::ABL1 (15). A later report also documented SH3-SH2 domain mutations in BCR::ABL1 (16). Although these regulatory domain mutations remain underexplored, their functional consequences demand thorough attention, considering their potential in altering responsiveness to TKI.

To address this gap, our study recruited a cohort of CML with clinically-confirmed resistance to first-line imatinib and interrogated mutational events beyond the KD, with particular emphasis on the regulatory SH2 and SH3 regions of BCR::ABL1. This analysis revealed a *de novo* mutation pair located within the SH2 (Y167H) and SH3 (T117P) domain. To elucidate the functional relevance of these alterations, we employed structure-guided *in silico* approaches to evaluate their impact on kinase conformation and drug binding. Molecular docking and molecular dynamics (MD) simulation indicated a destabilization of the imatinib-compatible conformation, predicting reduced inhibitor engagement. These computational insights were substantiated through a series of *in vitro* and *in vivo* experiments, which confirmed imatinib-resistance in presence of this mutation pair. Building on this, we further evaluated alternative TKIs to identify therapeutic strategies capable of overcoming this resistance phenotype. *In silico* analyses identified dasatinib as a potential second-line TKI (17). This prediction was further substantiated by *in vitro* and *in vivo* studies, which demonstrated robust restoration of drug sensitivity in presence of this mutation pair. Consistent with these findings, study cases harboring these alterations exhibited clinical benefit upon transition to dasatinib, supporting its therapeutic relevance in overcoming imatinib-resistance. Notably, the presence of this mutation pair in an independent validation cohort further strengthens the evidence that regulatory domain alterations in BCR::ABL1 may represent a previously under-appreciated mechanism of resistance in a subset of imatinib-refractory cases.

Results

Targeted deep sequencing reveals a de novo pair of mutations in SH2 and SH3 domain of BCR::ABL1 from imatinib-resistant CML cohort

To screen for the mutations in BCR::ABL1, we recruited a prospective identification cohort of imatinib-resistant CML (N = 37). The majority of cases (N = 27) were diagnosed in chronic phase (CP), while others in accelerated phase (AP) (N = 4) or blast crisis (BC) phase (N = 2) (**Supplementary Table S1**). Additionally, the majority was found to harbor e14-a2 variant of BCR::ABL1 (**Supplementary Fig. S2** and **Table S1**) (18). For mutation screening, we amplified a fragment of BCR::ABL1 which spanned from the exon 13 of BCR to the exon 10 of ABL1, encompassing their junction point, followed by SH3, SH2 and SH1 domain (schematic in Fig. 1A). Performing bidirectional targeted deep sequencing, we identified a *de novo* pair of mutations, T117P (nt. A496C) and Y167H (nt. T646C), in the SH3 and SH2 domain, respectively, in twelve cases (32%). (Fig. 1B, **Table 1**). Notably, six (16%) cases (CML02, CML07, CML12 CML17, CML23 and CML50) exclusively harbored this mutation pair, in absence of any candidate KD mutation (**Table 1**). In the remaining cases, this mutation pair co-occurred with candidate KD mutation, including, F359V (CML03), G250E (CML05), E255K (CML14), H396R (CML24) E459K (CML28) and L298V+E355G (CML48) (**Table 1**). Additionally, a single incidence (CML43) was found to only harbor the SH3 domain specific T117P mutation. To exclude the possibility that these two mutations represent any polymorphisms, we sequenced the corresponding ABL1 fragments from a group of healthy donors (N = 10), recruited from the study location, and, observed only wild-type sequence among them. However, a search of publicly available database identified Y167H as reported in the Catalogue Of Somatic Mutations In Cancer (COSMIC). Additionally, a previous study also reported the Y167H mutation in one of 94 imatinib-resistant cases (16). To the best of our knowledge, our study exclusively documented these two mutations occurring together, as a *de novo* pair, from an imatinib-resistant cohort.

Molecular modeling and simulation predict altered imatinib-response of BCR::ABL1 in presence of SH2–SH3 domain mutation pair

For interpreting drug-binding mechanisms in presence of this mutation pair, we performed *in silico* analyses of BCR::ABL1. In its inactive conformation, the Ramachandran plot showed 91.7% residues in the most favored regions, 8% in additionally allowed regions, and 0.3% in disallowed regions, with ERRAT quality factor 82.313 (**Supplementary Fig. S3, A and B**). For active conformation, the Ramachandran plot showed 89.4% residues in the most favored regions, 8% in additionally allowed regions, and 2.5% in generously allowed regions with no residues in disallowed regions. The ERRAT quality factor was 90.783 (**Supplementary Fig. S3, C and D**). Reportedly, in inactive conformation, the A-loop adopts a closed configuration that sterically blocks substrate access (19). The conserved DFG motif assumes a “DFG-out” position (20), flipping the Asp381 side chain away from catalytic center and disrupting coordination of Mg^{2+}, required for ATP binding (21). Concurrently, the αC-helix is rotated outward (αC-out), which breaks the essential Glu286-Lys271 salt bridge that stabilizes the active state (22). This inactive arrangement is further reinforced by intramolecular contacts between the SH3-SH2 domains and KD, which collectively impose an auto-inhibited conformation (19). In contrast, active conformation is characterized by a fully open A-loop that clears the substrate-binding site, a “DFG-in” positioning that aligns Asp381 for Mg^{2+} coordination, and an inwardly rotated αC-helix (αC-in) that re-forms the Glu286-Lys271 salt bridge. The SH2 domain reorients away from KD, relieving auto-inhibition and promoting

kinase activation. Notably, the gatekeeper residue Thr315 occupies an equivalent structural position in both states but contributes to shaping the ATP-binding pocket and modulating inhibitor access.

To assess the structural consequences of T117P and Y167H mutation on kinase activity, both the mutations were introduced into BCR::ABL1, in both active and inactive conformations, using PyMOL. For each mutation, the most favorable rotamers were selected, and steric clashes within a 5 Å radius of the mutated residues were resolved. The resulting mutated structures were subjected to energy minimization and extensive equilibration using a 500 ns molecular dynamics (MD) simulation in Desmond, to impose realistic conformational changes. Throughout the MD trajectory, the overall stability of the mutated protein was monitored by calculating the root-mean-square-deviation (RMSD) of the backbone atoms, which remained within ~ 3.5-4 Å at both active and inactive form of BCR::ABL1, indicating that the global conformation was maintained (**Supplementary Fig. S4A**) (23, 24). Root-means-square-fluctuation (RMSF) analysis of individual residues showed limited flexibility at both the proteins, with fluctuations below 4 Å for most regions (**Supplementary Fig. S4B**), suggesting that the forms of protein maintained structural integrity despite the presence of SH2 and SH3 domain-specific mutations.

Figure 2A represents a schematic of BCR::ABL1, starting with full length BCR construct, followed by SH3, SH2, ATP-binding and catalytic domain of ABL1. In the unphosphorylated condition, SH3 domain interacts with the linker region connecting the SH2 and N-terminal catalytic domain. In this catalytically-inactive auto-inhibited form, imatinib (in orange) binds perfectly with the enzyme. The T117 site, located at the SH3 domain, is distant to the imatinib-binding site. However, MD simulation showed that introduction of T117P significantly altered SH3-positioning, modifying its interaction with the SH2–linker interface (Fig. 2B). The combined model of T117P and Y167H mutation in SH3-SH2 assembled KD showed that the SH3 domain changes its position considerably in such a way that the intramolecular distance between the SH3 and SH2-linker interface is changed. This change altered the imatinib-binding site (Fig. 2B). We also carried out analysis of the Y167H mutant protein in its active conformation (Fig. 2C). Y167H mutation resides in the SH2 domain that does not have any direct consequences on the auto-inhibited conformation and is present on the solvent exposed site. But, in contrast, in the active conformation of the ABL protein (PDB ID: 1OPL), Y167H is close to SH2-linker interface. Upon mutation of Tyr167 on the active conformation, the SH2 domain shifted slightly away from the N-lobe, disrupting previously reported regulatory contacts (Fig. 2C). The mutation of Y167H in SH2 domain is more distantly located from the N-lobe, compared to wild-type protein, which breaks interaction with the top of N-lobe (Fig. 2D). Thus, the combined SH2–SH3 perturbation induced measurable conformational adjustments that reshaped the inactive conformation required for type II inhibitor binding.

The conformational states of BCR::ABL1 control the binding preferences of TKIs. Type II inhibitors, such as imatinib and nilotinib, selectively recognize the inactive “DFG-out” conformation (25), while type I inhibitors, such as dasatinib, target the active “DFG-in” state (26, 27). To understand the structural consequences of this mutation pair, we compared the modelled mutant proteins against their respective wild-type structures, in both inactive and active conformations. In the inactive conformation, a noticeable misalignment was observed in the SH3 and SH2 domains, indicating significant conformational

rearrangements driven by the mutations. These changes were particularly pronounced around the regions harboring the mutations, while the overall catalytic domain maintained a largely conserved fold (Fig. 3A). In the active conformation, a similar trend was observed, with the SH2 and SH3 domains showing structural deviations relative to the wild-type protein. Additionally, the A-loop of the mutant structure failed to align properly with the wild-type conformation (Fig. 3B), suggesting alterations in the regulatory elements that control kinase activation, while KD remained largely unchanged. These analyses established a stable structural framework of the mutated BCR::ABL1, suitable for subsequent docking studies with TKI agents.

The docking of imatinib to the wild-type inactive kinase reproduced the canonical binding mode observed in the co-crystal structure of ABL1 kinase (PDB: 2HYY). The ligand adopted a nearly planar conformation within the ATP-binding pocket, forming five conventional hydrogen bonds with Met318, Thr315, Asp381, and Ile360, in addition to π–π interactions with Phe382 and Tyr253 (Fig. 3C). The docking score of imatinib was − 14.127 kcal/mol. To verify the correct alignment of this docked conformation, we superimposed this onto the co-crystallized imatinib conformation, resulting in an RMSD of 0.335 Å, which also confirms the validity of the docking protocol. The alignment of imatinib-bound complex structures was represented in Fig. 3D. In contrast, docking of imatinib to the mutated inactive kinase revealed a significant shift in ligand orientation, with only a single hydrogen bond retained with Ala399 (Fig. 3E). The ligand was displaced toward the periphery of the pocket, and docking score increased to -3.349 kcal/mol, reflecting a substantial reduction in binding affinity. These results provide a structural explanation for the observed imatinib-resistance, demonstrating how the mutations allosterically perturb the inactive conformation, compromising inhibitor-binding.

The pair of SH3-SH2 domain mutations in BCR::ABL1 leads to imatinib-resistance

To test the imatinib-response of this mutation pair, cells from IL-3 dependent murine pro-B line, Ba/F3, were stably transfected with wild-type, T117P+Y167H-mutant or T315I-mutant (as control of imatinib-resistance) construct of BCR::ABL1 (**Supplementary Fig. S5, A and B**). Upon confirming IL3-independence of the cells, the expression of BCR::ABL1 was also verified (**Supplementary Fig. S5C**). Next, these three isogenic lines were comparatively measured for response to imatinib. Firstly, the colony forming ability was assessed by soft agar assay. As expected, imatinib treatment significantly inhibited colony formation from cells harboring wild-type BCR::ABL1 (Fig. 4A). On contrary, the same treatment minimally perturbed colony formation from cells harboring T117P+Y167H-mutant protein, similar to those with T315I-mutant (Fig. 4A). Next, the imatinib-sensitivity was tested by MTT assay. Expression of wild type BCR::ABL1 rendered sensitivity to imatinib in Ba/F3 cells, while T315I-mutant, as reported (6), showed resistance to the same (Fig. 4B). Interestingly, cells with T117P+Y167H-mutant BCR::ABL1 exhibited a prominent rise in IC_{50}, relative to the cells with wild-type protein (609 versus 300.4 nM), demonstrating reduced imatinib-response (Fig. 4B). Finally, we performed propidium iodide (PI) uptake assay to determine cellular viability. Following imatinib treatment, cells were measured by flow

cytometry and the results revealed a significantly lower number of PI + ve cells from the Ba/F3 line expressing T117P+Y167H- or T315I-mutant BCR::ABL1, compared to those with wild-type protein (Fig. 4C). Together, these data verified the loss of imatinib-response in presence of the SH3-SH2 domain mutation pair in BCR::ABL1.

To validate the efficacy of imatinib treatment, *in vivo* experiments were performed using NOD/SCID mice. Subcutaneous Ba/F3 xenografts were generated with above-mentioned isogenic Ba/F3 lines. Animals were subsequently treated with imatinib, as tumor reached a volume of ~ 100 mm^3 (Fig. 4D). The results revealed a significant decrease in tumor weight and volume in the set of wild-type BCR::ABL1 harboring mice (Fig. 4, E-G). Interestingly, tumors with T117P+Y167H-mutant BCR::ABL1 showed insignificant effect upon imatinib treatment, in comparison to wild-type counterparts and mirrored the phenotypic outcome from those with T315I mutation (Fig. 4, E-G). These findings confirmed the pathogenesis of imatinib-resistance in presence of the identified pair of SH3-SH2 domain mutations in BCR::ABL1.

BCR::ABL1 culminates its downstream effects through a signaling cascade, which lead to phosphorylation of STAT5 as a crucial mediator (26, 28). As reported (29), we found that imatinib abrogated STAT5-phosphorylation in cells harboring wild-type BCR::ABL1, in a dose- or time-dependent manner (**Supplementary Fig. S6, A-B**). Surprisingly, cells with T117P+Y167H-mutant BCR::ABL1, too, showed similar results. This was unlike the isogenic line harboring T315I-mutant BCR::ABL1, which, reportedly, showed minimal effects on phosphorylation-abrogation under the same condition (**Supplementary Fig. S6, A-B**). We tested this further with immunohistochemistry of *ex vivo* tumor specimens. Here too, the results showed abrogation of STAT5-phosphorylation in the tumors with T117P+Y167H-mutant BCR::ABL1, similar to those with wild-type protein (**Supplementary Fig. S6D**), suggesting alternative mechanism(s) for molecular pathogenesis of imatinib-resistance from SH3-SH2 domain mutant BCR::ABL1.

Dasatinib overcomes imatinib-resistance from SH3-SH2 domain mutant BCR::ABL1

To overcome this imatinib-resistance, we attempted *in silico* assessment with 2nd generation TKI agents, namely, dasatinib and nilotinib. The inactive conformation was used for the docking of nilotinib, consistent with its type II inhibitor binding mode, whereas the active conformation was used for dasatinib, a type I inhibitor that preferentially targets the DFG-in state. Dasatinib was docked to both the wild-type and T117P+Y167H-mutant BCR::ABL1, at its active conformation. Docking on the wild-type protein, at its catalytically-active conformation, reproduced the co-crystal binding pose observed in the PDB structure of c-Abl TK (PDB: 4XEY), with > 90% alignment of the ligand (RMSD = 0.626 Å) and docking score of -9.059 kcal/mol (Fig. 5A). Interestingly, in the mutated protein with active conformation, the docking score slightly increased to -5.854 kcal/mol, due to minor conformational adjustments of dasatinib within the binding site. Binding pattern analysis revealed that dasatinib maintained key interactions with the active site residues, including hydrogen bonds with Asp381, Glu286, Asn322, and

Leu248, as well as a halogen bond with Gly250 (Fig. 5B). Despite minor conformational flips in the mutated protein, the overall binding pattern remained highly similar to that of wild-type, reflecting robust and stable occupancy of the active site. In contrast to dasatinib, docking of nilotinib to the mutated protein, showed partial retention of the canonical binding site interactions. Hydrogen bonding and hydrophobic π–π interactions with Phe382 were observed, although the ligand was slightly displaced toward a smaller sub-pocket (Fig. 5C). The docking score of -5.613 kcal/mol indicates moderate binding affinity. This evaluation led us to select dasatinib, as chosen TKI, to test its efficacy against SH3-SH2 domain mutant BCR::ABL1.

Subsequently, the above-mentioned isogenic Ba/F3 lines were assayed by a set of experiments. Firstly, the effect of dasatinib on colony-forming ability of cells, was tested using soft agar assay. Compared to the cells harboring T315I-mutant protein, those with T117P+Y167H-mutant BCR::ABL1 showed decreased number of colonies upon dasatinib treatment (Fig. 6A). We found this feature similar to those with wild-type protein, indicating the sensitivity of SH3-SH2 domain mutant BCR::ABL1 to dasatinib. Next, MTT assay was performed and the results revealed a significant decrease of IC_{50} values from cells harbouring T117P+Y167H-mutant BCR::ABL1, in comparison to those with wild-type counterpart (0.45 versus 0.73 nM) (Fig. 6B). As reported (30–32), cells with T315I-mutant BCR::ABL1, showed significantly less response to dasatinib (IC_{50}, 14.69 nM). Additionally, PI uptake assay also supported that SH3-SH2 domain mutant BCR::ABL1 responds to dasatinib (Fig. 6C).

To confirm the clinical potential of dasatinib, on SH3-SH2 domain mutant BCR::ABL1, we performed *in vivo* analyses with NOD-SCID mice. Tumors, from subcutaneously injected Ba/F3 cells, were treated with dasatinib or vehicle (Fig. 6D). The observations revealed that tumors with T117P+Y167H-mutant BCR::ABL1, showed higher sensitivity to dasatinib, in comparison to tumors with wild-type protein, whereas the tumors with T315I-mutant BCR::ABL1, as reported (31), showed non-responsiveness to dasatinib (Fig. 6, E-G). Tumor volume and size, both, showed significant reduction upon dasatinib treatment in presence of SH3-SH2 domain mutant BCR::ABL1. Additionally, the sensitivity of dasatinib was also confirmed from phospho-STAT5 levels. Immuno-blotting of Ba/F3 cells (**Supplementary Fig. S7A**) and immunohistochemistry of *ex vivo* tumor specimens (**Supplementary Fig. S7B**), both showed reduction of STAT5-phosphorylation in presence of dasatinib, thus indicating the abrogation of signalling cascade upon BCR::ABL1 blockage. Together, these data validated the efficacy of dasatinib to overcome the imatinib-resistance from the identified pair of SH3-SH2 domain mutations in BCR::ABL1.

Clinical evidence supports the efficacy of dasatinib on the SH3-SH2 domain mutant BCR::ABL1

The experimental validation of dasatinib to overcome imatinib-resistance from SH3-SH2 domain mutations in BCR::ABL1, led us to scrutinize the follow-up information of concerned cases from the study cohort. We found a few interesting observations, as depicted schematically in Fig. 6H. A case (CML02), exclusively bearing this mutation pair, were advised dasatinib in April 2024, as second-line TKI,

and we noted a favorable survival outcome in latest follow-up of January 2026. Another case (CML14), who harbors this mutation pair with co-occurring KD mutation, E255K, is under dasatinib regimen since May 2019 and we noted a successful outcome, latest in January 2026. We would also highlight a third case (CML17), exclusively bearing this mutation pair, is under nilotinib regimen since July 2019 and has shown favorable outcome till latest follow-up in January 2026. MD simulation predicted partial binding ability of nilotinib for SH3-SH2 domain mutant BCR::ABL1, in our experimental set-up, and we found its efficacy from this case study.

Additionally, we tested a separate cohort (N = 6) of imatinib-resistant cases, where deep sequencing found this mutation pair in one individual (16.7%) (**Supplementary Table S2**), further validating the incidence of SH3-SH2 domain mutations in BCR::ABL1.

Discussion

Screening of targetable KD mutations in BCR::ABL1, referred as IRMA (Imatinib-Resistance-Mutation-Analysis), is a common diagnostic practice upon front-line TKI-resistance in CML. The presence of targetable mutation leads to selection of next-generation TKI, as second-line treatment (33). The problem arises with cases who showed no targetable KD mutation. This sub-cohort is referred as 'BCR::ABL1 kinase-independent TKI-resistance' and they show poorer outcome than cases with 'BCR::ABL1 kinase-dependent TKI-resistance' (8, 9, 34, 35). Their management often depends on 3rd - generation TKI, ponatinib, which can target alternative signaling cascades or combinatorial approaches (35). Indeed, the latest 2025 European Leukemia Net (ELN) guidelines did not specify any separate regimen for this sub-cohort (36).

The conformation and function of any TK family members are regulated by SH2 and SH3 domain (37, 38). In the context of cellular ABL (cABL), these two domains create an auto-inhibitory, inactive state of the protein by clamping as allosteric inhibitor (12, 39, 40). ABL1, when fused with BCR at N-terminus, also maintain this regulation (41). Indeed, imatinib irreversibly blocks the protein at its inactive conformation, thus preventing its conversion to enzymatically active and functional conformation (41). Imatinib binds to BCR::ABL1 at its ATP-binding site in KD and thus, acts as ATP-inhibitor (41). KD mutation, which disrupts this binding, initiates imatinib-resistance. Importantly, the conformation of the catalytic pocket of BCR::ABL1 depends on SH2 and SH3 domain. Thus, mutational changes in any of these domains might disrupt the same and potentially block imatinib to access BCR::ABL1. While we conducted the screening for KD mutations in an imatinib-resistant CML cohort (N = 37), we observed a sub-cohort of cases (N = 11, 29.7%) with no candidate KD mutation, previously reported in (42). However, deep sequencing of domains outside KD, revealed a pair of mutations, from SH2 and SH3 domain, respectively, in five cases of this sub-cohort. Additionally, we also found this mutation pair to co-occur with candidate KD mutation in a number of cases. While we searched the literature for SH3-SH2 domain mutations in CML, we found earlier studies where *in vitro* mutagenesis and structural modeling revealed the potential of SH3-SH2 domain mutations, to disrupt imatinib-competent inactive conformation of BCR::ABL1 (11, 43, 44). Further support came from a clinical trial which recorded imatinib-resistance in

cases with BCR::ABL1 mutations outside KD region (45). Subsequently, an elegant study from the group of Michael W. Deininger validated the relevance of SH3-SH2 domain mutations from a CML cohort with imatinib-resistance (15). Despite this, very little data are reported, thereafter, on the same. One such report documented four candidate SH2 and SH3 domain mutations from a CML cohort (16). To note, they reported SH2 domain specific Y167H mutation in one of 94 cases. However, in our study, interestingly, we found Y167H to co-occur with T117P mutation in SH3 domain, among imatinib-resistant cases. Subsequently, we tested the effect of these mutations on imatinib-binding. Based on MD simulation showing altered binding, we proceeded for *in vitro* testing where assays revealed reduced cellular response to imatinib. Xenograft studies, subsequently, confirmed the reduced efficacy of imatinib for BCR::ABL1 harboring this mutation pair. Together, this study identified a pair of SH3-SH2 domain mutations of BCR::ABL1 in pathogenesis of imatinib-resistance, highlighting the importance of the regulatory regions, beyond BCR::ABL1 KD, as pathogenic driver. However, to confirm non-responsiveness of T117P+Y167H-mutant BCR::ABL1 to imatinib, surprisingly, we found no effect on STAT5-phosphorylation. To note, JAK/STAT5 signaling cascade is downstream of BCR::ABL1, along with RAS/RAF/MAPK and PI3K/AKT/mTOR pathways (26, 28). Our observation led us to deduce that SH3-SH2 domain mutant BCR::ABL1 might engage separate signaling pathway(s), to be explored in future.

To overcome imatinib-resistance from candidate BCR::ABL1 KD mutations, several next generation TKIs are clinically available (46). Interestingly, we found a clinical trial (NCT00064233) documenting dasatinib to overcome imatinib-resistance in cases harboring SH2 (S157R and Y174C) and SH3 (V90A and E98G) domain mutations (45). This strengthened our selection of dasatinib as MD simulation revealed its unperturbed affinity for BCR::ABL1 with the SH3-SH2 domain mutation pair. Separately, another second-generation TKI, nilotinib showed partial affinity for the mutant protein, in comparison to wild-type BCR::ABL1. Aided with *in silico* prediction, we proceeded for *in vitro* and *in vivo* testing of dasatinib efficacy and both the systems verified the same. Dasatinib, indeed, showed higher efficacy to mutant BCR::ABL1 from wild-type protein, in our study set-up. Though, at present, we could not dissect this higher efficacy, nonetheless, we are convinced to propose dasatinib as a drug of choice in case SH3-SH2 domain mutations block imatinib to target BCR::ABL1. Moreover, our study emphasizes the need of including SH2 and SH3 domains with existing panel of BCR::ABL1 KD mutation screening. This revised panel shall not only broaden up the list of targetable mutations of BCR::ABL1; this shall save more imatinib-resistant cases with a next-generation TKI.

Materials/Subjects and Methods

Cohort recruitment

Imatinib-resistant CML cases were recruited with signed consent, from Saroj Gupta Cancer Centre & Research Institute, Kolkata, India (identification cohort), N.R.S Medical College and Hospital, Kolkata, India, Balco Medical Centre, Raipur, India, and, AIIMS, New Delhi, India (validation cohort) under the approval of Institutional Human Ethics Committee (IHEC). Ph + ve Primary CML cases with front-line

imatinib-resistance marked the inclusion criterion (details in (42)). Clinico-pathological data were recorded and blood specimen were collected from recruited cases.

RNA isolation and cDNA synthesis

This was done as described previously (42).

PCR amplification

This was performed as described previously (42)(details in **Supplementary methods)**.

Deep sequencing

The PCR products were purified and subjected to targeted-deep sequencing using Illumina paired-end MiSeq 300 platform, according to manufacturer's protocol. Data analyses were executed as described previously (42).

Molecular dynamics (MD) simulation:

Point mutations were introduced into wild-type protein using PyMOL and resulting mutated structures were subjected to a 500 ns molecular dynamics (MD) simulation in Desmond (details in **Supplementary methods)**.

Cell culture and treatment

Ba/F3 cells were maintained in RPMI-1640 medium with 10% fetal bovine serum, 100 U/mL penicillin, and 100 µg/mL streptomycin at 37°C under 5% CO_2, in presence of recombinant murine interleukin-3 (IL-3) (PeproTech, Cat No: 213 − 13).

Plasmid construction and site-directed mutagenesis

Plasmid MSCV-BCR-ABL-IRES-GFP (Addgene) was used as source of wild-type BCR::ABL1 and point mutations (T117P, Y167H or T315I) were introduced using Q5 Site-Directed Mutagenesis Kit (New England Biolabs), according to manufacturer's instructions. All constructs were verified by Sanger sequencing. Plasmids, amplified in *E coli* DH5α strain, were purified using endotoxin-free plasmid isolation kit (Macherey-Nagel).

Electroporation and generation of stable line

Cells were transfected with plasmid by electroporation. Exponentially growing $1x10^7$ cells were harvested, washed, and re-suspended in cytomix buffer [120 mM KCl, 0.15 mM $CaCl_2$, 10 mM K_2HPO_4/KH_2PO_4 (pH 7.6), 25 mM HEPES, 2 mM EGTA, and 5 mM MgCl, (pH 7.6)]. Plasmid (5 µg) was added to the cell suspension, following electroporation at 260 V/950µF (Gene Pulser, Biorad). Upon immediately transferring to pre-warmed complete RPMI medium, cells were allowed to recover under

standard culture condition. Cells were selected upon removing IL3 from the culture media post 48 h of transfection.

MTT assay

Cells, in triplicate, were plated and treated with 500 nM imatinib/1 nM dasatinib/vehicle control for 48 h. Subsequently, 3-(4,5-dimethylthiazol-2-yl)-2,5-diphenyltetrazolium bromide (MTT; Himedia) was added for 4 h and upon solubilizing in DMSO (SRL), absorbance was measured at 570 nm. Cell viability was expressed as a percentage, relative to vehicle control.

Soft agar assay

Petri dishes, in triplicate, were overlaid with 0.6% base agar (Sigma-Aldrich) in complete RPMI media. Cells (5×10^3 cells/$35mm^3$) were re-suspended in 0.3% agar in complete RPMI media and overlaid on base agar, in presence of 500 nM Imatinib/1 nM dasatinib/vehicle control for 21 days. Images were taken using Nikon ECLIPSE Ti2 inverted microscope. Colonies were counted by ImageJ and plotted using GraphPad Prism version 9.0.

Propidium Iodide (PI)-uptake assay

Cells, in triplicate, were treated with 500 nM imatinib/1 nM dasatinib/vehicle control for 48 h. Upon harvesting, cells were stained with PI (0.1 µg/ml; Sigma-Aldrich) and assayed using BD FACSCanto II Flow Cytometer. Data were analyzed using FCS Express 7.

Western blot (WB)

WB was performed as described previously (47). Membranes were probed with antibodies against c-Abl (sc-23, Santa Cruz Biotechnology), phospho-Stat5 (Tyr694) and Stat5 (#9359 and #94205, Cell Signalling Technology), and, α-tubulin (Proteintech). Following incubation with DyLight™ conjugated secondary antibody (Thermo Fisher Scientific), blots were viewed on Odyssey CLx Imaging System (LiCor Inc.)

Murine xenograft model

Animal experiments were conducted in accordance with institutional ethical guidelines and approved protocols. Six to eight-week-old NOD-SCID mice (N = 5/set, 3 male & 2 female) were subcutaneously injected with cells (0.5×10^6 cells/mouse) into the right flank. At tumor volume of 100 mm^3 (day 12), imatinib (in PBS) or dasatinib (in 80 mM Citrate buffer, pH 3.0–3.1) (HY-50946 and HY-10181, MedChemExpress) was treated via intra-peritoneal injection, with imatinib at 50 mg/kg/alternative day for 10 days and dasatinib at 10 mg/kg daily for 7 days.

Immunohistochemistry (IHC)

Tumors were harvested, and, formalin fixed and paraffin embedded. IHC was performed as described previously (47) with primary antibody against phospho-Stat5 (Tyr694) and Stat5 (#9359 and #94205, Cell Signalling Technology). Images were obtained with Leica DM750 light microscope.

Statistical analysis

Data are presented as mean ± standard deviation. Statistical analyses were performed using appropriate statistical tests as specified in the figure legends. p-value < 0.05 was considered statistically significant.

Declarations

Competing Interests:

Authors declare no competing financial interests related to the works described.

Author Contributions:

SD, AT, SN conceived the hypothesis and designed the study. AT, MKS, SN supervised the study. DB, DD, DP, RD, TKD recruited and evaluated the cohort. SD, KS, SB performed *ex vivo* experiments. SP performed *in silico* experiments. SD, RM performed *in vitro* and *in vivo* experiments. SD, RM, SP, AT, MKS, SN analysed the data. SD, RM, SP, AT, SN drafted the manuscript. SN secured the research funding.

Acknowledgements:

This study was supported by the grant-in-aid (0097/RND/BIOSCI/Nil/Jan-21/1/1), Dept. of Science, Technology and Biotechnology (DSTBT)- Govt. of West Bengal, and, the Institutional Research Grant (Application Number: 3330, year 2021), Lady Tata Memorial Trust awarded to Somsubhra Nath. The Ba/F3 line was a kind gift from Prof. Anita Chopra, AIIMS, New Delhi. We acknowledge Dr. Amitava Sengupta, CSIR-IICB, Kolkata, and, Dr. Mayukh Biswas, Institute of Health Sciences, Presidency University, Kolkata, for providing cell culture reagents.

Data Availability Statement:

The raw data of sequencing are available from the corresponding author on request.

References

1. Rowley JD (1973) A New Consistent Chromosomal Abnormality in Chronic Myelogenous Leukaemia identified by Quinacrine Fluorescence and Giemsa Staining. Nature 243(5405):290–293. 10.1038/243290a0
2. Lugo TG, Pendergast AM, Muller AJ, Witte ON (1990) Tyrosine Kinase Activity and Transformation Potency of *bcr-abl* Oncogene Products. Science 247(4946):1079–1082. 10.1126/science.2408149
3. Jabbour E, Kantarjian H (2024) Chronic myeloid leukemia: 2025 update on diagnosis, therapy, and monitoring. Am J Hematol 99(11):2191–2212. 10.1002/ajh.27443

4. Hochhaus A, Larson RA, Guilhot F, Radich JP, Branford S, Hughes TP et al (2017) Long-Term Outcomes of Imatinib Treatment for Chronic Myeloid Leukemia. N Engl J Med 376(10):917–927. 10.1056/NEJMoa1609324
5. Kamizela AE, Leongamornlert D, Williams N, Wang X, Nyamondo K, Dawson K et al (2025) Timing and trajectory of BCR::ABL1-driven chronic myeloid leukaemia. Nature 640(8060):982–990. 10.1038/s41586-025-08817-2
6. Gorre ME, Mohammed M, Ellwood K, Hsu N, Paquette R, Rao PN et al (2001) Clinical Resistance to STI-571 Cancer Therapy Caused by BCR-ABL Gene Mutation or Amplification. Science 293(5531):876–880. 10.1126/science.1062538
7. Soverini S, Hochhaus A, Nicolini FE, Gruber F, Lange T, Saglio G et al (2011) BCR-ABL kinase domain mutation analysis in chronic myeloid leukemia patients treated with tyrosine kinase inhibitors: recommendations from an expert panel on behalf of European LeukemiaNet. Blood 118(5):1208–1215. 10.1182/blood-2010-12-326405
8. Rinke J, Hochhaus A, Ernst T (2020) CML - Not only BCR::ABL1 matters. Best Pract Res Clin Haematol 33(3):101194. 10.1016/j.beha.2020.101194 PubMed PMID: 33038988
9. Cruz-Rodriguez N, Torres-Llanos Y, Deininger MW (2026 Feb) Intrinsic cellular resistance to BCR::ABL1 inhibitors. Haematologica 12. 10.3324/haematol.2025.287814 PubMed PMID: 41676916
10. Smith KM, Yacobi R, Van Etten RA (2003) Autoinhibition of Bcr-Abl through Its SH3 Domain. Mol Cell 12(1):27–37. 10.1016/S1097-2765(03)00274-0
11. Azam M, Latek RR, Daley GQ (2003) Mechanisms of Autoinhibition and STI-571/Imatinib Resistance Revealed by Mutagenesis of BCR-ABL. Cell 112(6):831–843. 10.1016/S0092-8674(03)00190-9
12. Lorenz S, Deng P, Hantschel O, Superti-Furga G, Kuriyan J (2015) Crystal structure of an SH2–kinase construct of c-Abl and effect of the SH2 domain on kinase activity. Biochem J 468(2):283–291. 10.1042/BJ20141492
13. Panjarian S, Iacob RE, Chen S, Engen JR, Smithgall TE (2013) Structure and Dynamic Regulation of Abl Kinases*. J Biol Chem 288(8):5443–5450. 10.1074/jbc.R112.438382
14. Rossari F, Minutolo F, Orciuolo E (2018) Past, present, and future of Bcr-Abl inhibitors: from chemical development to clinical efficacy. J Hematol Oncol 11(1):84. 10.1186/s13045-018-0624-2
15. Sherbenou DW, Hantschel O, Kaupe I, Willis S, Bumm T, Turaga LP et al (2010) BCR-ABL SH3-SH2 domain mutations in chronic myeloid leukemia patients on imatinib. Blood 116(17):3278–3285. 10.1182/blood-2008-10-183665 PubMed PMID: 20519627; PubMed Central PMCID: PMC2995357
16. Vaidya S, Vundinti BR, Shanmukhaiah C, Chakrabarti P, Ghosh K (2015) Evolution of BCR/ABL Gene Mutation in CML Is Time Dependent and Dependent on the Pressure Exerted by Tyrosine Kinase Inhibitor. Buday L, editor. PLoS ONE. ;10(1):e0114828. 10.1371/journal.pone.0114828
17. Lindauer M, Hochhaus A, Dasatinib (2018) Recent Results Cancer Res 212:29–68. 10.1007/978-3-319-91439-8_2 PubMed PMID: 30069624
18. Salmon M, White HE, Zizkova H, Gottschalk A, Motlova E, Cerveira N et al (2022) Impact of BCR::ABL1 transcript type on RT-qPCR amplification performance and molecular response to

therapy. Leukemia 36(7):1879–1886. 10.1038/s41375-022-01612-2 PubMed PMID: 35676453; PubMed Central PMCID: PMC9252903

19. Nagar B, Hantschel O, Young MA, Scheffzek K, Veach D, Bornmann W et al (2003) Structural basis for the autoinhibition of c-Abl tyrosine kinase. Cell 112(6):859–871. 10.1016/s0092-8674(03)00194-6 PubMed PMID: 12654251
20. Tokarski JS, Newitt JA, Chang CYJ, Cheng JD, Wittekind M, Kiefer SE et al (2006) The Structure of Dasatinib (BMS-354825) Bound to Activated ABL Kinase Domain Elucidates Its Inhibitory Activity against Imatinib-Resistant ABL Mutants. Cancer Res 66(11):5790–5797. 10.1158/0008-5472.CAN-05-4187
21. Shan Y, Seeliger MA, Eastwood MP, Frank F, Xu H, Jensen MØ et al (2009) A conserved protonation-dependent switch controls drug binding in the Abl kinase. Proc Natl Acad Sci USA 106(1):139–144. 10.1073/pnas.0811223106
22. Levinson NM, Kuchment O, Shen K, Young MA, Koldobskiy M, Karplus M et al (2006) A Src-Like Inactive Conformation in the Abl Tyrosine Kinase Domain. Pawson T, editor. PLoS Biol. ;4(5):e144. 10.1371/journal.pbio.0040144
23. Kundu B, Sarkar D, Chowdhuri SP, Pal S, Das SK, Das BB et al (2020) Development of a metabolically stable topoisomerase I poison as anticancer agent. Eur J Med Chem 202:112551. 10.1016/j.ejmech.2020.112551
24. Pal S, Ghosh Dastidar U, Ghosh T, Ganguly D, Talukdar A (2022) Integration of Ligand-Based and Structure-Based Methods for the Design of Small-Molecule TLR7 Antagonists. Molecules 27(13):4026. 10.3390/molecules27134026
25. Manley PW, Cowan-Jacob SW, Fendrich G, Strauss A, Vapai N, Grzesiek S et al (2006) Bcr-Abl Binding Modes of Dasatinib, Imatinib and Nilotinib: An NMR Study. Blood 108(11):747–747. 10.1182/blood.V108.11.747.747
26. Quintás-Cardama A, Cortes J (2009) Molecular biology of BCR::ABL1–positive chronic myeloid leukemia. Blood 113(8):1619–1630. 10.1182/blood-2008-03-144790
27. Laurini E, Posocco P, Fermeglia M, Gibbons DL, Quintás-Cardama A, Pricl S (2013) Through the open door: Preferential binding of dasatinib to the active form of BCR-ABL unveiled by *in silico* experiments. Mol Oncol 7(5):968–975. 10.1016/j.molonc.2013.06.001
28. Amarante-Mendes GP, Rana A, Datoguia TS, Hamerschlak N, Brumatti G (2022) BCR::ABL1 Tyrosine Kinase Complex Signaling Transduction: Challenges to Overcome Resistance in Chronic Myeloid Leukemia. Pharmaceutics 14(1):215. 10.3390/pharmaceutics14010215 PubMed PMID: 35057108; PubMed Central PMCID: PMC8780254
29. Nam S, Williams A, Vultur A, List A, Bhalla K, Smith D et al (2007) Dasatinib (BMS-354825) inhibits Stat5 signaling associated with apoptosis in chronic myelogenous leukemia cells. Mol Cancer Ther 6(4):1400–1405. 10.1158/1535-7163.MCT-06-0446 PubMed PMID: 17431118
30. Shah NP, Tran C, Lee FY, Chen P, Norris D, Sawyers CL (2004) Overriding imatinib resistance with a novel ABL kinase inhibitor. Science 305(5682):399–401. 10.1126/science.1099480 PubMed PMID:

15256671

31. Soverini S, Colarossi S, Gnani A, Castagnetti F, Rosti G, Bosi C et al (2007) Resistance to dasatinib in Philadelphia-positive leukemia patients and the presence or the selection of mutations at residues 315 and 317 in the BCR-ABL kinase domain. Haematologica 92(3):401–404. 10.3324/haematol.10822 PubMed PMID: 17339191
32. O'Hare T, Walters DK, Stoffregen EP, Jia T, Manley PW, Mestan J et al (2005) *vitro* Activity of Bcr-Abl Inhibitors AMN107 and BMS-354825 against Clinically Relevant Imatinib-Resistant Abl Kinase Domain Mutants. Cancer Res 65(11):4500–4505. 10.1158/0008-5472.CAN-05-0259
33. Oehler VG, Berman E, Huang IJ (2026) Management of chronic myeloid leukemia with tyrosine kinase inhibitors: adverse events, toxicities and therapy dosing. haematol. 12. 10.3324/haematol.2025.288334
34. Braun TP, Eide CA, Druker BJ (2020) Response and Resistance to BCR::ABL1-Targeted Therapies. Cancer Cell 37(4):530–542. 10.1016/j.ccell.2020.03.006
35. Loscocco F, Visani G, Galimberti S, Curti A, Isidori A (2019) BCR-ABL Independent Mechanisms of Resistance in Chronic Myeloid Leukemia. Front Oncol 9:939. 10.3389/fonc.2019.00939
36. Apperley JF, Milojkovic D, Cross NCP, Hjorth-Hansen H, Hochhaus A, Kantarjian H et al (2025) 2025 European LeukemiaNet recommendations for the management of chronic myeloid leukemia. Leukemia 39(8):1797–1813. 10.1038/s41375-025-02664-w
37. Pawson T, Gish GD, Nash P (2001) SH2 domains, interaction modules and cellular wiring. Trends Cell Biol 11(12):504–511. 10.1016/s0962-8924(01)02154-7 PubMed PMID: 11719057
38. Koch CA, Anderson D, Moran MF, Ellis C, Pawson T (1991) SH2 and SH3 domains: elements that control interactions of cytoplasmic signaling proteins. Science 252(5006):668–674. 10.1126/science.1708916 PubMed PMID: 1708916
39. Corbi-Verge C, Marinelli F, Zafra-Ruano A, Ruiz-Sanz J, Luque I, Faraldo-Gómez JD (2013) Two-state dynamics of the SH3–SH2 tandem of Abl kinase and the allosteric role of the N-cap. Proc Natl Acad Sci USA 110(36). 10.1073/pnas.1303966110
40. Lamontanara AJ, Georgeon S, Tria G, Svergun DI, Hantschel O (2014) The SH2 domain of Abl kinases regulates kinase autophosphorylation by controlling activation loop accessibility. Nat Commun 5(1):5470. 10.1038/ncomms6470
41. Irgit A, Kamıs R, Sever B, Tuyun AF, Otsuka M, Fujita M et al (2025) Structure and Dynamics of the ABL1 Tyrosine Kinase and Its Important Role in Chronic Myeloid Leukemia. Arch Pharm 358(5):e70005. 10.1002/ardp.70005
42. Dey S, Basu S, Shah S, Bhattacharyya D, Gupta PP, Acharjee M et al (2022) Deep sequencing reveals the spectrum of BCR::ABL1 mutations upon front-line therapy resistance in chronic myeloid leukemia: An Eastern-Indian cohort study. Cancer Treat Res Commun 33:100635. 10.1016/j.ctarc.2022.100635
43. Barilá D, Superti-Furga G (1998) An intramolecular SH3-domain interaction regulates c-Abl activity. Nat Genet 18(3):280–282. 10.1038/ng0398-280

44. Hantschel O, Nagar B, Guettler S, Kretzschmar J, Dorey K, Kuriyan J et al (2003) A Myristoyl/Phosphotyrosine Switch Regulates c-Abl. Cell 112(6):845–857. 10.1016/S0092-8674(03)00191-0
45. Talpaz M, Shah NP, Kantarjian H, Donato N, Nicoll J, Paquette R et al (2006) Dasatinib in Imatinib-Resistant Philadelphia Chromosome–Positive Leukemias. N Engl J Med 354(24):2531–2541. 10.1056/NEJMoa055229
46. Haddad FG, Jabbour EJ, Gutkin SW, Pathak AK, Zhai Y, Kantarjian HM (2026) BCR::ABL1 Mutational Profiling in US Patients With Chronic-phase Chronic Myeloid Leukemia on Tyrosine Kinase Inhibitors. CDP 6(2):186–198. 10.21873/cdp.10518
47. Roy S, Saha S, Dhar D, Chakraborty P, Singha Roy K, Mukherjee C et al (2022) Molecular crosstalk between CUEDC2 and ERα influences the clinical outcome by regulating mitosis in breast cancer. Cancer Gene Ther 29(11):1697–1706. 10.1038/s41417-022-00494-x PubMed PMID: 35732909

Tables

Table 1 is available in the Supplementary Files section.

Figures

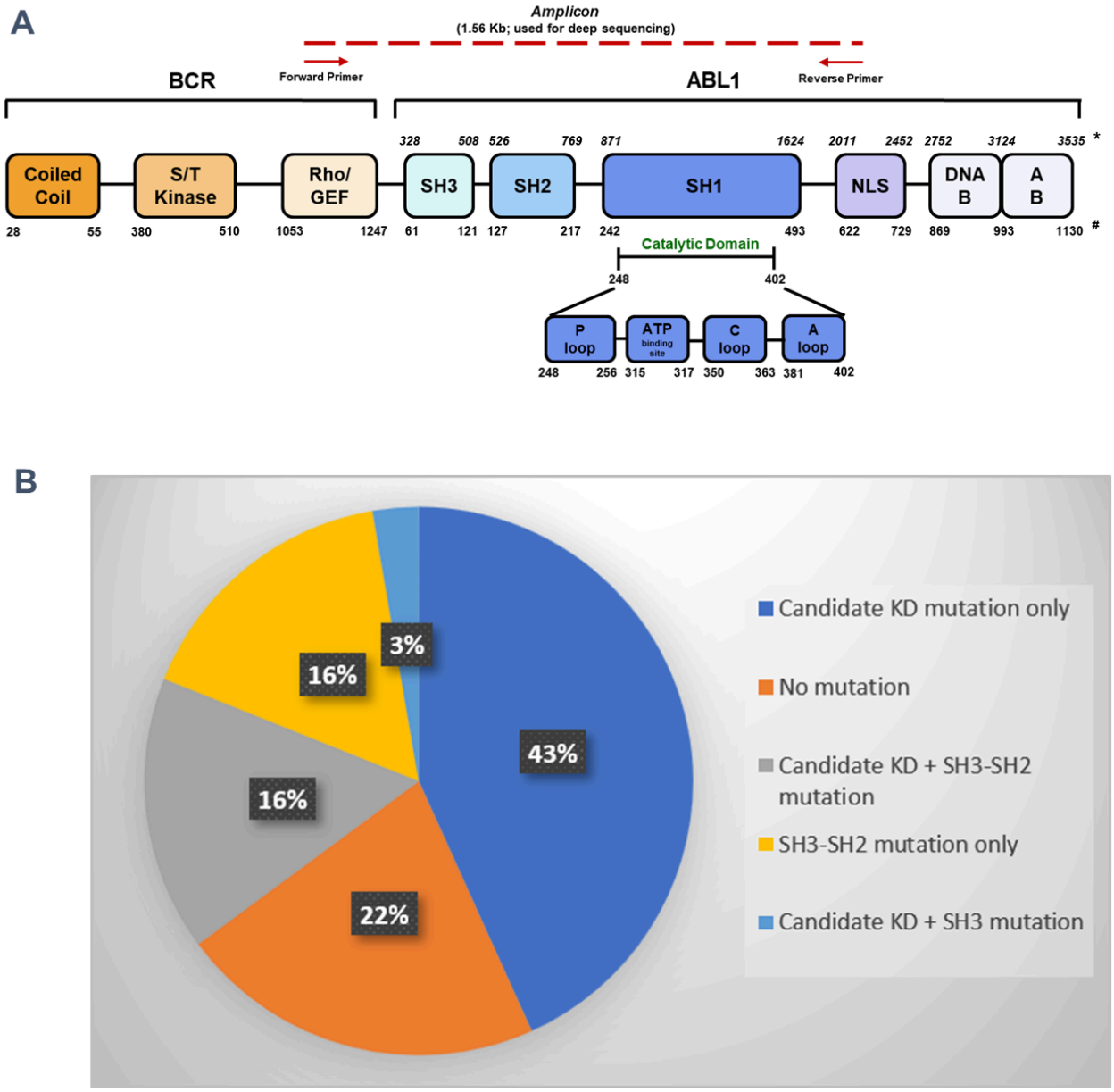


Figure 1

Mutation analysis of BCR::ABL1 from study cohort, by targeted deep sequencing. **(A)** Schematic of BCR-ABL1 fusion protein. Corresponding domains are depicted. The PCR amplicon and corresponding primers are marked. *, nucleotide position (according to GenBank Accession No. x16416.1); #, amino acid position. **(B)** Pie diagram showing the frequency of cases with candidate kinase domain (KD) mutations only, SH3-SH2 domain mutation pair or both. A single case with SH3 domain-specific T117P

mutation with KD-specific M244V was also documented. Cases without KD or SH3-SH2 domain mutations were documented as ‘no mutation’.

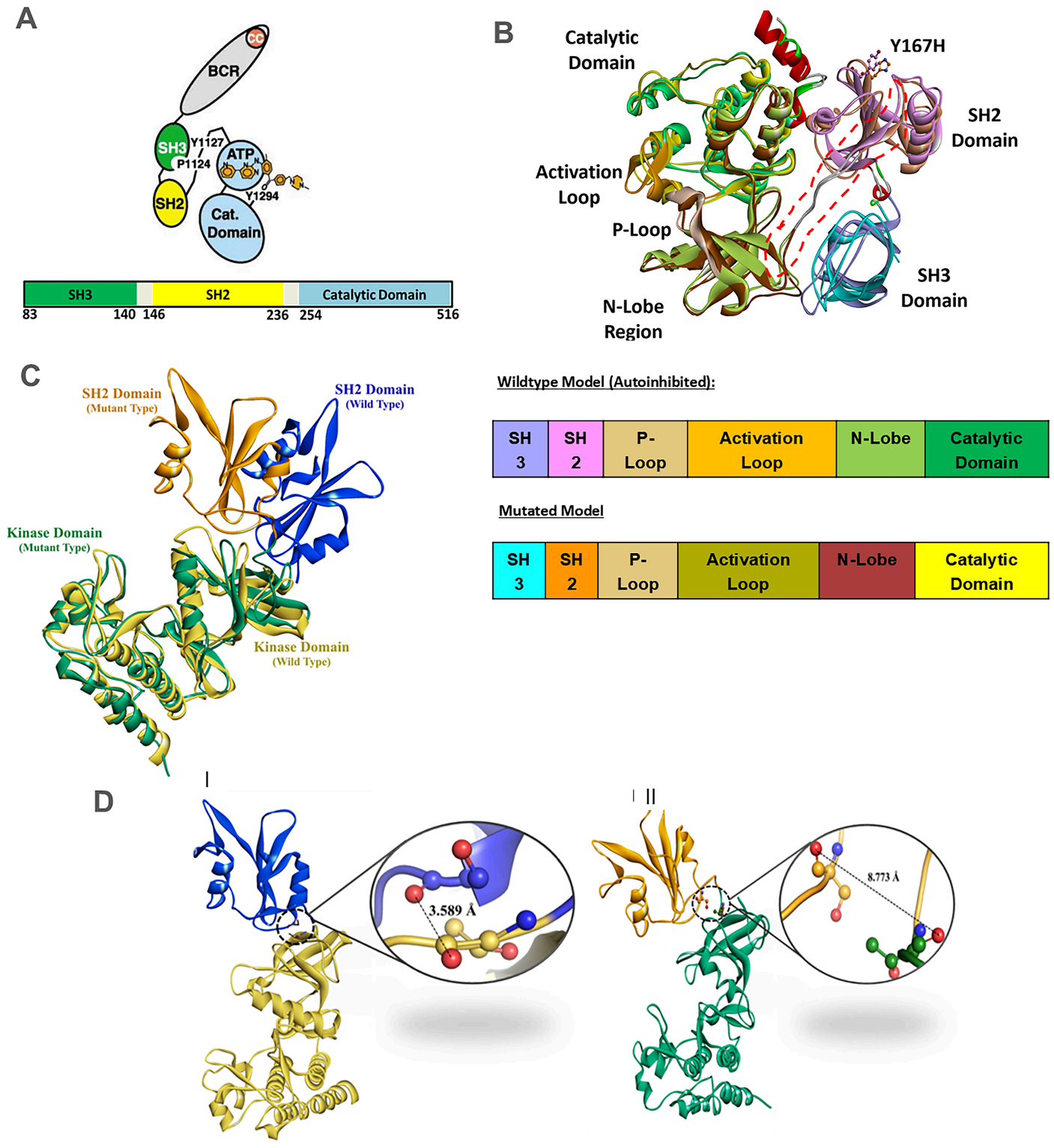


Figure 2

The impact of SH3-SH2 domain mutation pair on the structural organization of BCR::ABL1. **(A)** Schematic of BCR::ABL1 showing domain structures. Imatinib (shown in orange line representation)

binds on the ATP binding site of the catalytic domain. **(B)** Structural overlapping of wild type and Y167H-mutant BCR::ABL1, in its auto-inhibited (inactive) conformation. Mutated residue (Y167H) is depicted in stick representation. Other domains in both proteins are depicted by different colored cartoon representations. Changed conformation in N-lobe SH2 linker regions are marked by red dotted line. **(C)** Compensatory mutation analysis of the Y167H mutant in the active conformation of ABL1 (PDB : 1OPL). Mutation is located near the interface between SH2 domain (Blue) and kinase domain (Yellow) in the active conformation of wild-type ABL1. The conformational changes of the mutant SH2 domain and kinase domain are displayed by orange and green cartoon representation. **(D)** (In left) Position of SH2 domain (Blue) and kinase domain (Yellow) along with their intermediate distance in the wild type protein; (In right) After mutation (Y167H), position of SH2 domain changes which increases the intermediate distance between SH2 domain (Orange) and kinase domain (Green).

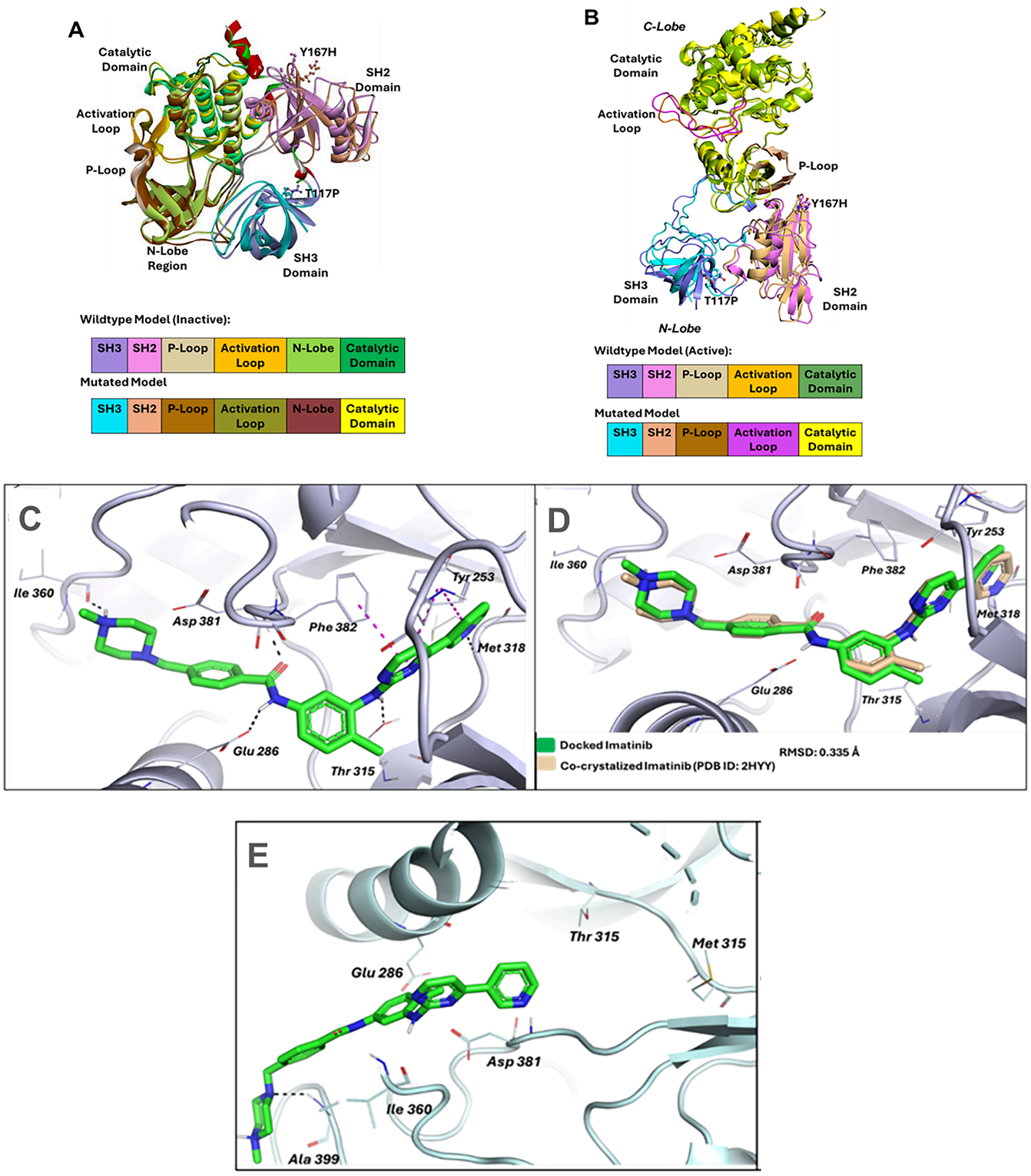


Figure 3

The impact of SH3-SH2 domain mutation pair on imatinib-binding affinity of BCR::ABL1. (**A-B**) Impact of the presence of T117P and Y167H mutations on the inactive (**A**) and active (**B**) conformation of BCR::ABL1. Domains and significant motifs of the proteins are mentioned and depicted in different colors. (**C**) Binding interaction of imatinib on the wild-type inactive conformation of BCR::ABL1. Imatinib is represented by green stick representations whereas the protein is represented by grey cartoon

representations. Black dotted line indicates the hydrogen bond and magenta dotted line indicates the π-π hydrophobic interaction. (**D**) Structural alignment of imatinib docked conformations (green stick) with co-crystalized imatinib conformations (yellow stick) (**E**) Binding interaction of imatinib on the mutated inactive conformation of BCR::ABL1. Imatinib is represented by green stick representation and the protein is represented by grey cartoon representations. Black dotted line indicates the hydrogen bond.

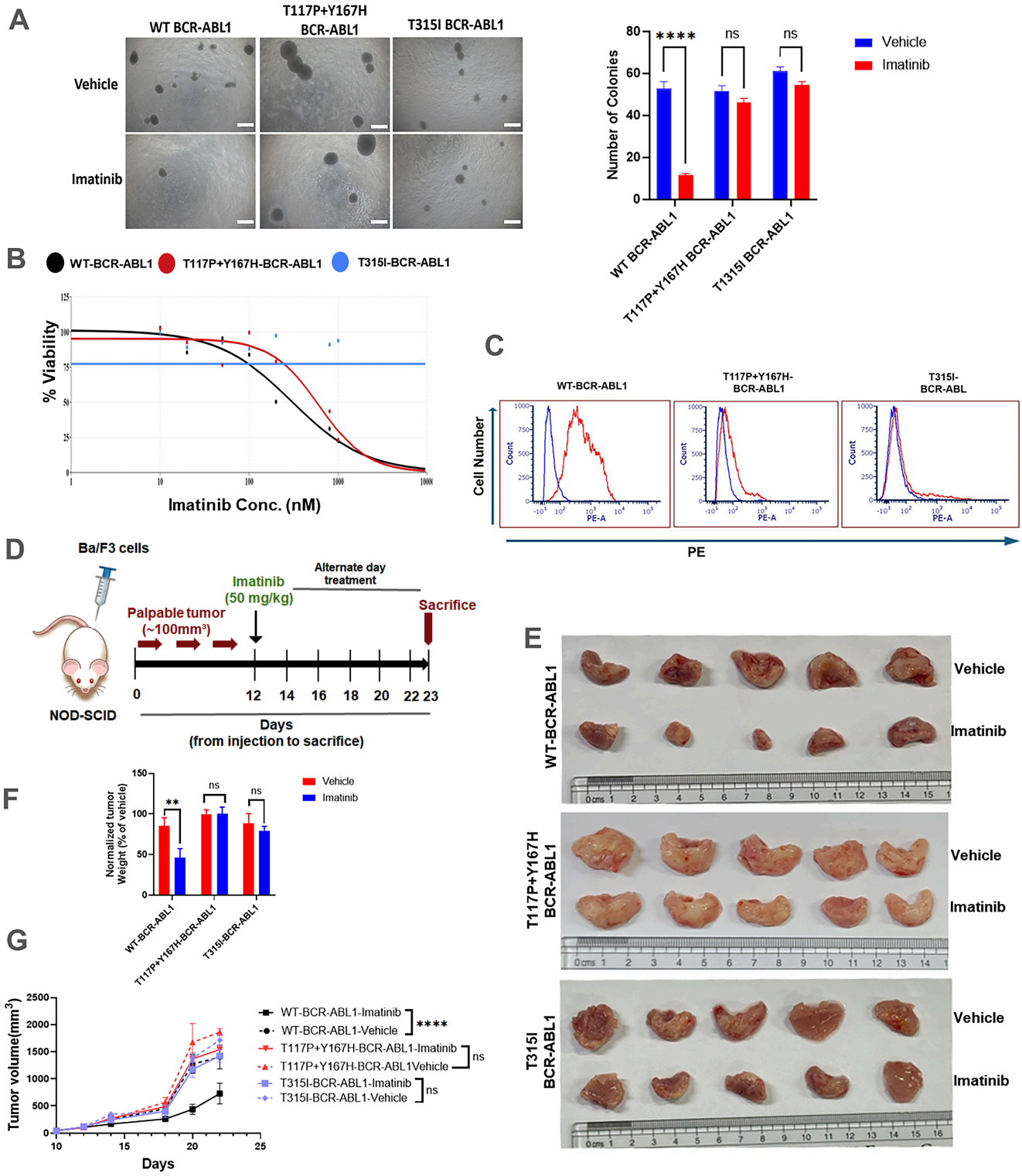


Figure 4

The SH3-SH2 domain mutation pair in BCR::ABL1 leads to imatinib-resistance. **(A-C)** Ba/F3 cells, harboring wild-type (WT), T117P+Y167H- and T315I-mutant BCR::ABL1 were treated with vehicle or imatinib (500 nM). (A) Soft agar colony formation assay was performed. The representative microscopic image was shown (at day 21) and values of triplicate experiments were plotted. *, p-value <0.05; ns, non-significant p-value. (B) MTT assay was performed following 48 h of treatment and values were plotted. **(C)** PI-uptake assay was performed following 96 h of treatment and data was shown. Blue line indicates the untreated control; red line indicates the treated condition. **(D)** Schematic of xenograft experimentation. Corresponding days of treatment module were indicated. Animals were sacrificed at day 23. **(E-G)** NOC-SCID mice (N=5/condition) were injected with 0.5 x 10^6 Ba/F3 cells, harboring wild-type (WT), T117P+Y167H- and T315I-mutant BCR::ABL1 and treated as mentioned in (D). Photographs of tumors, harvested from each set, were shown **(E)**, and, normalized tumor weight (% of vehicle-treated condition) **(F)** and volume (in mm^3) **(G)** were plotted. **, p-value <0.005; **** p-value <0.00005; ns, non-significant p-value.

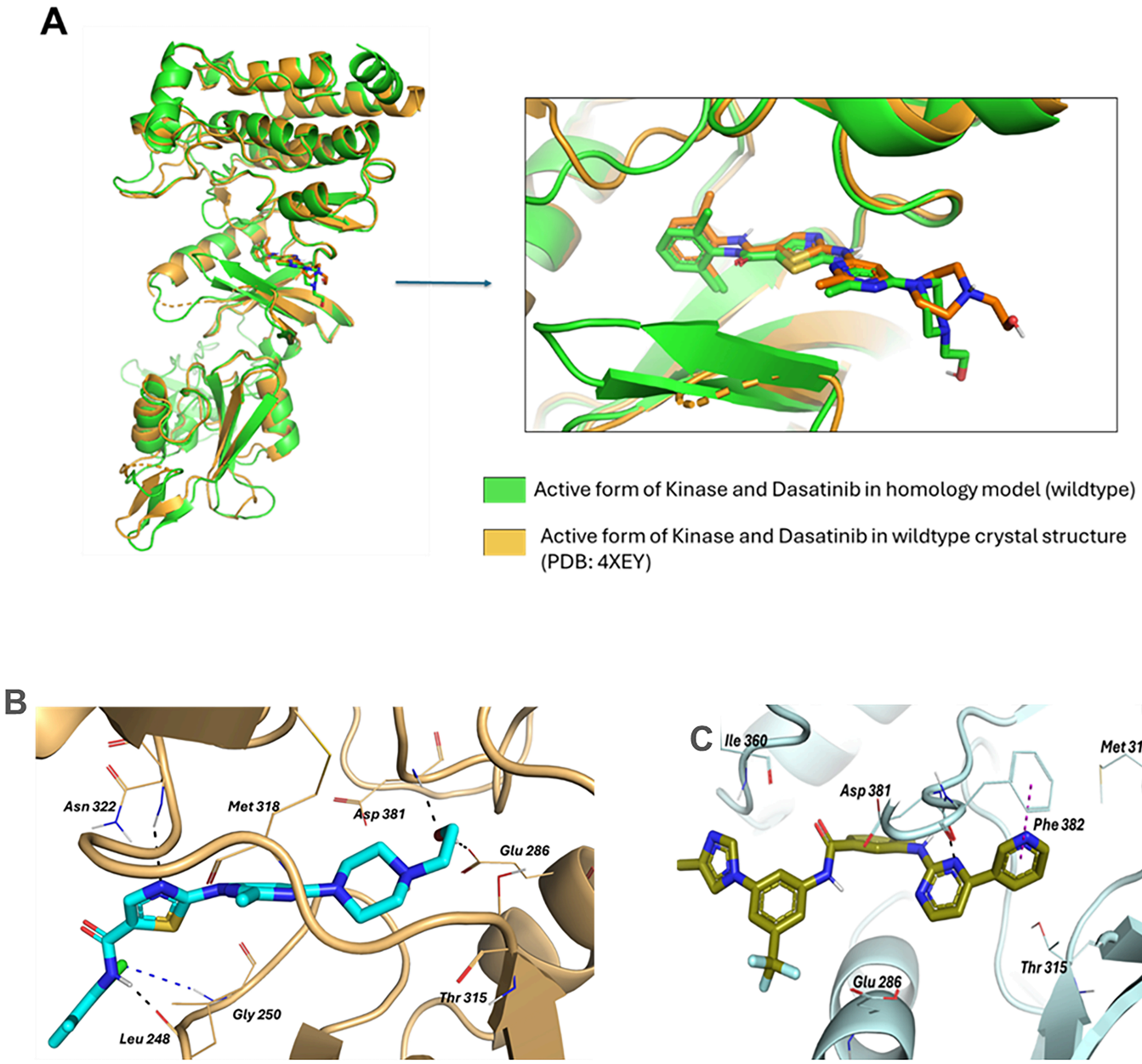


Figure 5

Binding potential of dasatinib and nilotinib to SH3-SH2 domain mutant BCR::ABL1. (**A**) Superimposed structures of the docked dasatinib–BCR::ABL1 complex with the wild-type active kinase co-crystallized with dasatinib (PDB: 4XEY). The docked Dasatinib is shown in green stick representation, while the co-crystallized dasatinib is shown in orange. (**B**) Binding interactions of Dasatinib with the mutated active conformation of BCR::ABL1. Dasatinib is shown in cyan stick representation, and the protein in grey cartoon representation. Black dotted lines indicate hydrogen bonds, while blue dotted lines indicate halogen bond interactions. **(C)** Binding interaction of nilotinib on the mutated inactive conformation of BCR::ABL1. Nilotinib is represented by olive color stick representation, and the protein is represented by grey cartoon representations. Black dotted line indicates the hydrogen bond, and magenta dotted line indicates the π-π hydrophobic interaction.

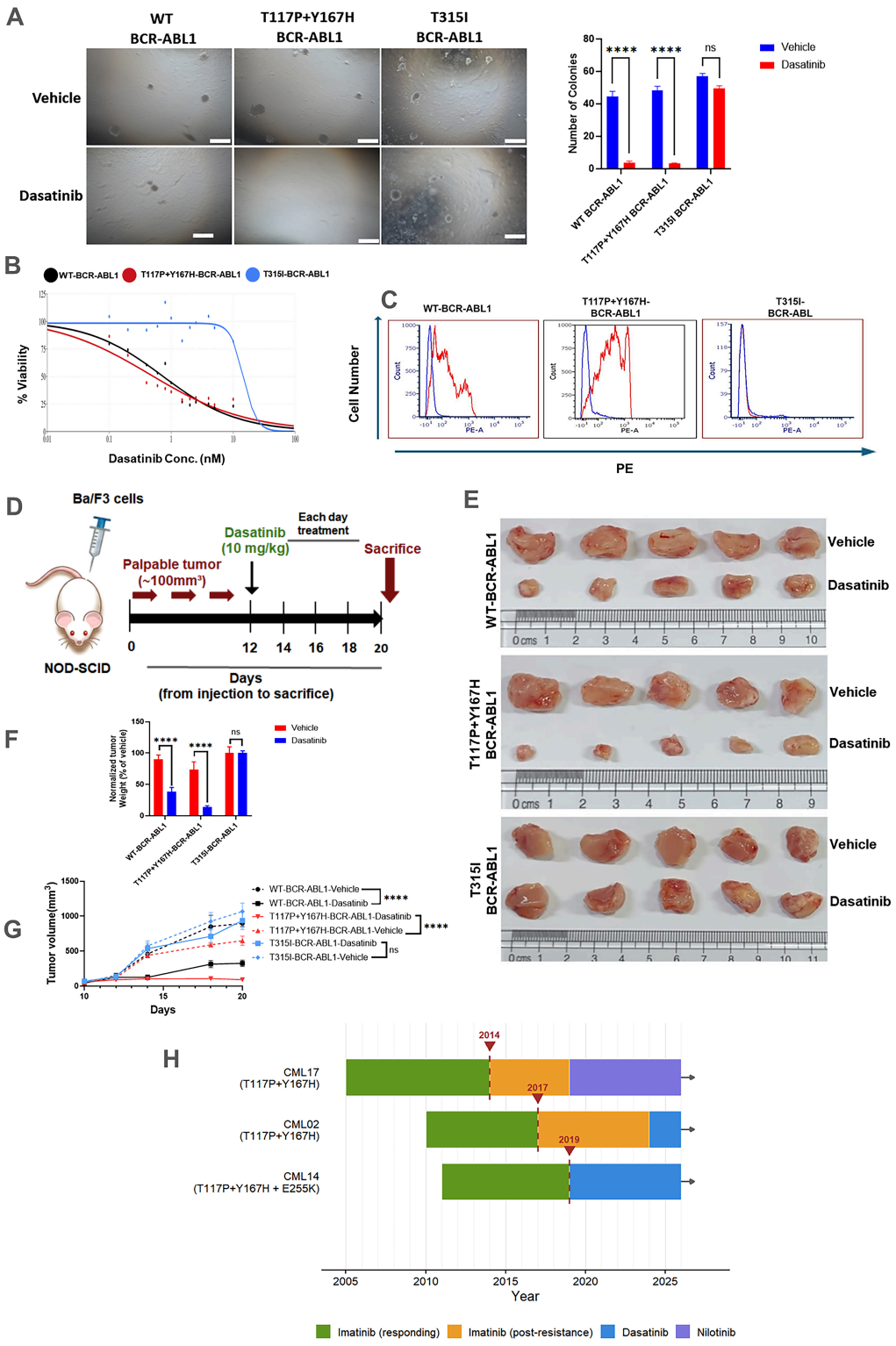


Figure 6

Dasatinib overcomes imatinib-resistance from SH3-SH2 domain mutant BCR::ABL1. **(A-C)** Ba/F3 cells, harboring wild-type (WT), T117P+Y167H- and T315I-mutant BCR::ABL1 were treated with vehicle or dasatinib (100 nM). (A) Soft agar colony formation assay was performed. The representative microscopic image was shown (at day 21) and values of triplicate experiments were plotted. *, p-value <0.05; ns, non-significant p-value. (B) MTT assay was performed following 48 h of treatment and values

were plotted. **(C)** PI-uptake assay was performed following 48 h of treatment and data was shown. Blue line indicates the untreated control; red line indicates the treated condition. **(D)** Schematic of xenograft experimentation. Corresponding days of treatment module were shown. Animals were sacrificed at day 20. **(E-G)** NOC-SCID mice (N=5/condition) were injected with 0.5 x 10^6 Ba/F3 cells, harboring wild-type (WT), T117P+Y167H- and T315I-mutant BCR::ABL1 and treated as mentioned in (D). Photographs of tumors, harvested from each set, were shown **(E)**, and, normalized tumor weight (% of vehicle-treated condition) **(F)** and volume (in mm^3) **(G)** were plotted. **** p-value <0.00005; ns, non-significant p-value.

Supplementary Files

This is a list of supplementary files associated with this preprint. Click to download.

- Table1.docx
- SupplementaryFigureS1.jpg
- SupplementaryFigureS2.jpg
- SupplementaryFigureS3.jpg
- SupplementaryFigureS4.jpg
- SupplementaryFigureS5.jpg
- SupplementaryFigureS6.jpg
- SupplementaryFigureS7.jpg
- SupplementaryfileSupplementarymethodsSupplementaryfiguretablelegends.docx
- SupplementaryTableS1.docx
- SupplementaryTableS2.docx
- SupplementaryTableS2.docx